Monograph:
Nehmzow, U., Akanyeti, O. and Billings, S.A. (2009) Towards modeling complex robot training tasks through system identification. Research Report. ACSE Research Report no. 993 . Automatic Control and Systems Engineering, University of Sheffield

Towards Modeling Complex Robot Training tasks Through System Identification

Ulrich Nehmzow[1], O Akanyeti[1],and S A Billings[2]
[1]Dept Computer Science, University of Ulster, Ireland
[2]Dept Automatic Control and Systems Engineering, University of Sheffield

Department of Automatic Control and Systems Engineering
The University of Sheffield, Sheffield, S1 3JD, UK

Research Report No. 993

June 2009

Towards Modelling Complex Robot Training Tasks through System Identification

U. Nehmzow[1], O. Akanyeti[2] and S.A. Billings[3]
[1] *School of Computing and Intelligent Systems, University of Ulster, UK.*
[2] *Department of Computer Science, University of Essex, UK.*
[3] *Department of Automatic Control and Systems Engineering, University of Sheffield, UK.*

Abstract

Previous research has shown that sensor-motor tasks in mobile robotics applications can be modelled *automatically*, using NARMAX system identification, where the sensory perception of the robot is mapped to the desired motor commands using non-linear polynomial functions, resulting in a tight coupling between sensing and acting — the robot responds *directly* to the sensor stimuli without having internal states or memory.

However, competences such as for instance sequences of actions, where actions depend on each other, require memory and thus a representation of state. In these cases a simple direct link between sensory perception and the motor commands may not be enough to accomplish the desired tasks. The contribution to knowledge of this paper is to show how fundamental, simple NARMAX models of behaviour can be used in a bootstrapping process to generate *complex* behaviours that were so far beyond reach.

We argue that as the complexity of the task increases, it is important to estimate the current state of the robot and integrate this information into the system identification process. To achieve this we propose a novel method which relates distinctive locations in the environment to the state of the robot, using an unsupervised clustering algorithm. Once we estimate the current state of the robot accurately, we combine the state information with the perception of the robot through a bootstrapping method to generate more complex robot tasks: We obtain a polynomial model which models the complex task as a function of predefined low level sensor motor controllers and raw sensory data.

The proposed method has been used to teach *Scitos G5* mobile robots a number of *complex* tasks, such as advanced obstacle avoidance, or complex route learning.

1. Introduction

Fundamentally, the behaviour of a robot is a result of the interaction of three factors: i) the robot's hardware, ii) the robot's controller, and iii) the environment the robot is operating in. The robot acquires information from the environment through its sensors, which provides the input signals to the controller. The controller computes the desired motor commands and the robot performs these commands in the environment to achieve the desired task [1].

Given that sensing and the actions of a robot are coupled dynamically, given the sensitivity of robot sensor's to slight changes in the environment, robot-environment interaction exhibits complex, non-linear, often chaotic and usually unpredictable characteristics [2,3]. Because of this, the task of robot programming — designing a control program to achieve a desired behaviour — is difficult. Unlike other engineering disciplines, there is no formal, theory-based design methodology which the robot programmer can follow to program a robot to achieve a desired task.

Nevertheless, we have previously shown that the robot programming process *can* be automated: sensor-motor competences in mobile robotics applications can be modelled automatically and algorithmically, using robot training and system identification methods. The stages of our method are summarized below:

(i) Acquisition of a training data set. First the programmer demonstrates the desired behaviour to the robot via driving it manually [4,5] or direct human demonstration [6,7]. During this run, sensory perception and the desired velocity commands of the robot are logged. There is a considerable corpus of robotics research on robot training, for example training by verbal instructions [8], using expectations [9] or imitation of a human trainer [10]. This work on robot training is relevant to the experiments presented here, in that the same method of acquiring training data is used, but the focus of our experiments is not on training, but on automatically obtaining low-level be-

haviours and, again automatically, combining these into more complex behaviours, without the need to have dedicated robot programming skills.

(ii) Pre-processing of input signals. Having thus obtained the raw training data, we preprocess the input signals to reduce the dimensionality of the input space [11] and also to identify the important sensory readings, which are highly correlated with the desired motor commands [12].

(iii) Model estimation. We then model the relationship between the encoded sensory perception and the actions of the robot using ARMAX (Auto-Regressive Moving Average models with eXogenous inputs) [13,14] and NARMAX (Non-linear ARMAX) [15,16] system identification methods. These techniques are supervised parameter estimation methodologies for identifying both the important model terms and the parameters of unknown non-linear dynamic systems. They produce linear or non-linear polynomial functions to model the input-output relationship. A single model is usually enough to identify the whole relationship successfully.

(iv) Model validation and optimization. Once the sensor-based controllers are obtained, they are used to drive the robot in the target environment to validate their performances. Also at this stage, it is sensible to carry out sensitivity analysis [17,18] in order to estimate the influence of individual sensor readings upon the robot's global behaviour [19,6]. This would help us to determine which parameters in the model contribute the most to output variability and which parameters are insignificant and can be eliminated from the final model, leading to more parsimonious models.

(v) Analytical analysis of the obtained models. The representation of the task as a transparent, analysable polynomial model simplifies the identification of the important factors that affect the robot's behaviour. For instance, the error reduction ratio gives an indication of the importance of individual model terms. Likewise, variance-based methods of sensitivity analysis [18,20,21] or entropy-based methods [22] allow the identification of important input components (e.g. sensors).

1.1. *Motivation: From Simple to Complex Tasks*

The method described above has been successfully applied to generate various sensor-motor tasks, from simple behaviours, such as wall following [4] or door traversal [19], to some complicated behaviours, such as following a moving object [23] and path learning [11].

However as the complexity of task increases, representing the whole relationship between sensory perception and the desired motor responses of the robot in one single model using only raw sensory inputs would lead to large models. Training such models is extremely difficult, and obtained models often exhibit brittle performance.

The novel contribution of this paper is to show how the NARMAX system identification method can be used to model more *complex* robot training tasks, such as tasks where sensor-motor couplings change along a path, or depending on circumstance. To do so, we focus on two fundamental ideas:

(i) For complex tasks, the actions of the robot depend not only on raw sensory perception, but also on the current state of the robot. Therefore there is a need to represent the present state of the robot, and to incorporate it into the model.

(ii) As our goal is to simplify the robot programming process such that non-programmers can generate robot control code, there is still need for a simple method to generate the motor commands that take the robot from one state to another, accomplishing the desired task.

In this paper, we address both issues with a general overlook. In Section 2 we focus on the state transition problem, and propose a novel method relating the state of the robot to distinctive objects seen in the environment: First, the robot learns to recognize landmarks in the environment, using standard classification techniques. Once the robot is capable of localising, using these landmarks, it obtains a different sensor-motor coupling for each recognized landmark.

After estimating which state the robot is in, the next step is to combine the state information with the perception of the robot in a general framework to generate the essential motor commands in order to accomplish the desired complex robot training tasks.

In Section 3, we therefore introduce a bootstrapping method of generating complex robot training tasks using polynomial NARMAX models. The method is based on obtaining hierarchical polynomial models which model the desired task by combining predefined low level sensor-motor controllers, raw sensory data and state inputs.

2. State Estimation Through Unsupervised Learning

In complex tasks it is often the case that the relationship between perception and the motor response varies along the robot's path. We deal with this situation, using two stages:

In the first stage the robot clusters the environment in to subspaces using standard classification techniques (SOM, K-means, etc.) based on its own sensory perception. Note that here we assume that state transitions can be observed by the robot through its sensors. Then in the second stage it obtains a model for each cluster separately using system identification techniques (Figure 1).

With this method, state transitions are related to robot-environment interaction, which allows the robot to identify the state changes automatically, using its own perception. In this paper, the K-means algorithm is used as a classifier,

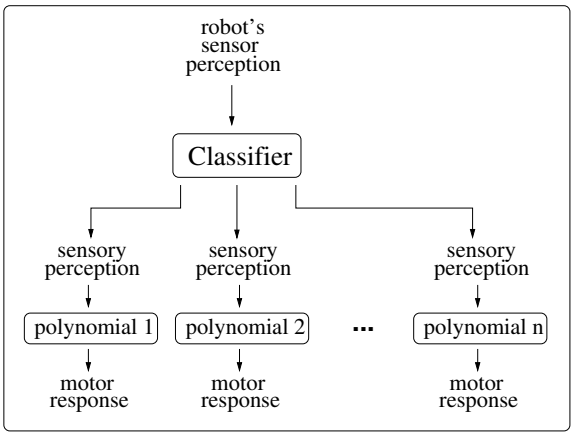

Fig. 1. The proposed method to cope with the state transition problem while generating robot control programs: a classifier divides the perception-action space of the robot into subspaces, and generates a separate model for each subspace.

described in Section 2.1.

It might be instructive at this point to refer briefly to the work done on simultaneous localisation and mapping (SLAM). SLAM focusses on precise robot localisation, using adaptive filtering techniques such as Kalman filters and Bayesian methods [24], and is a more sophisticated method of robot self-localisation than simple clustering of a robot's sensory perception. We use the clustering to divide the input space to our system identification process, not to localise *precisely*, i.e. we do not perform SLAM in the experiments presented here.

2.1. *The K-means Classifier*

The k-means algorithm [25] is an unsupervised clustering algorithm which is used to classify a given data set into k clusters. The main idea is to define one centroid for each cluster and the algorithm attempts to satisfy two conditions: i) each class has a center which is the mean position of all the samples in that class and ii) each sample is in the class whose center it is closest to.

The algorithm starts by partitioning the input points into k initial sets, either at random or using some heuristic. It then calculates the mean point (centroid) of each set. A new partitioning of the data is achieved by associating each point with its closest centroid. The centroids are then recalculated for the new clusters, and the algorithm repeated until convergence, which is obtained when the points no longer switch clusters (or centroids are no longer changed).

2.2. *Robot Experiments: Experimental Setup*

We tested the proposed approach by teaching a *SCITOS G5* autonomous mobile robot to perform two different sensor-motor competences: right wall following and route learning. The experiments were conducted in the 100 square meter circular robotics arena of the University of Essex. The arena is equipped with a Vicon motion tracking system which can deliver position data (x, y and z), using reflective markers and high speed, high resolution cameras. The tracking system is capable of sampling the motion up to 100 Hz with an accuracy of better than 0.1 mm.

The robot is equipped with a Hokuyo laser range finder, facing the direction of travel, which delivers distance readings up to 4 m. This range sensor has a wide angular range (240°) with a radial resolution of 0.36° and distance resolution of less than 1 cm. The base of the robot is circular and and the diameter of the base is 60 cm.

2.3. *Experiment 1: Wall Following*

The first experiment presents result about teaching a robot to achieve right wall following behaviour. First, the programmer drives the robot in the training environment manually, using a joystick to demonstrate the desired wall following behaviour to the robot (Figure 2). During this run, the laser readings l_i and the motor commands (v and ω) of the robot were logged in every 250 ms to obtain the training data set.

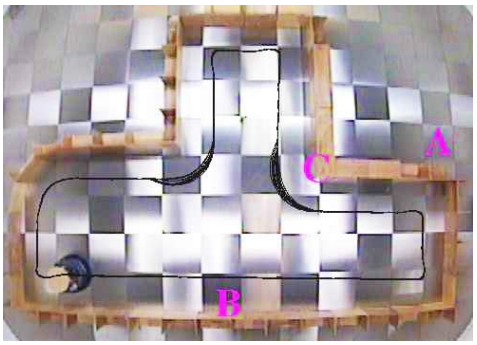

Fig. 2. Experiment 1. The trajectory of the robot under the control of the programmer demonstrating the desired right wall following behaviour.

Classifying the Robot's Perception Once the training data set was obtained, we coarse-coded the laser readings into 11 sectors by averaging 62 readings for each 22° intervals, in order to decrease the dimensionality of the input space to the K-means algorithm. Coarse-coded laser readings larger than 1.5 m were clamped to 1.5 m, so that during classification the robot would only take into account nearby objects.

We then used the K-means algorithm to recognize 3 distinctive regions (regions A, B and C) in the training environment, using the 11-dimensional laser perception of the robot. It turns out that region A represents the concave corners, region B represents the straight walls and region C represents the convex corners in the environment.

Figure 3 shows the graphical illustration of the three centroids. The analysis of the figure reveals that for convex corners (region C), laser readings of the robot are high except from the right side. Contrarily for concave corners (region A), the robot has small laser readings this time except from the left side. And for straight walls (region B)

the front readings of the robot also have high values since there is no wall in front of the robot.

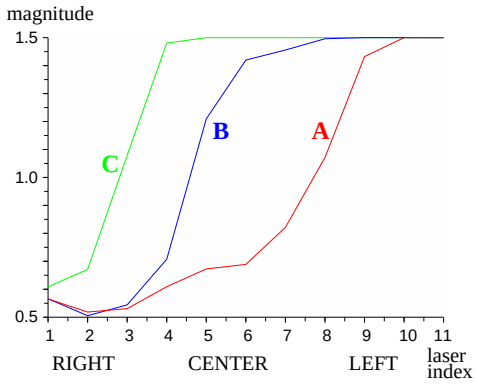

Fig. 3. Experiment 1. The graphical representation of the three centroids for regions A, B and C given in Table 3.

Once the robot gets a new laser signature (11-dimensional vector, $u_1 - u_{11}$) from the environment, the K-means classifier computes the Euclidean distance d_i between the new signature and the three centroids (Equation 1). The smaller the Euclidean distance, the higher the similarity between the laser perception and the class, therefore the laser perception is allocated to the class with the smallest Euclidean distance. Figure 4 shows how the robot classifies the environment along the route.

$$d_i = \sum_{j=1}^{11} l_{ij} - u_j \qquad i = 1, 2, 3 \qquad (1)$$

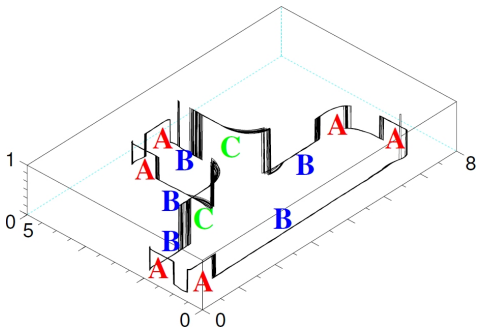

Fig. 4. Experiment 1. The internal map of the robot along the trajectory of the wall following behaviour.

Obtaining Perception-Action Models Having classified the environment into 3 regions, the next step was to model the relationship between the sensory perception of the robot and the desired motor responses using the NARMAX system identification technique for each region separately. To decrease the input dimensionality to the NARMAX models, the coarse-coded laser readings were reduced into a two-element input vector ($\hat{u}_1$ and $\hat{u}_2$), where $\hat{u}_1$ is the minimum coarse-coded laser reading among all the coarse-coded readings, and $\hat{u}_2$ is the rightmost coarse-coded laser reading in the signature.

For each region, two ARMAX models were obtained; one for the translational velocity (v) and one for the angular velocity (ω). The results are given in Table 1.

$v_A(n) = +0.001 + 0.198 \cdot \hat{u}_1$
$\omega_A(n) = +1.459 - 2.936 \cdot \hat{u}_1 - 0.632 \cdot \hat{u}_2$
$v_B(n) = -0.002 + 0.205 \cdot \hat{u}_1$
$\omega_B(n) = +0.979 - 1.980 \cdot \hat{u}_1$
$v_C(n) = +0.002 + 0.196 \cdot \hat{u}_1 - 0.400 \cdot \hat{u}_2$
$\omega_C(n) = +0.182 - 0.510 \cdot \hat{u}_1$

Table 1
Experiment 1. The three ARMAX models for the angular and linear speed of the robot for each identified region, to achieve wall following behaviour.

Model Validation Having obtained the sensor-based controllers, we let them drive the robot in the train environment. During the test run, first the K-means algorithm is used to recognize the location of the robot along the trajectory, and then to select the polynomial modelled for that particular region to drive the robot. The results showed that the robot is able to follow the wall accurately without losing the track or bumping into the walls (Figure 5).

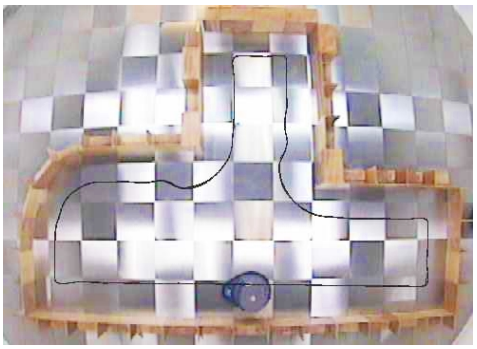

Fig. 5. Experiment 1. The trajectory of the robot under the control of three ARMAX models given in Table 1.

2.4. *Experiment 2: Route Learning*

The second experiment is more complex than the first one. Here, the robot has to follow a particular route in a more complex environment, where the causal relationship between the sensory perception of the robot and the motor responses varies along the trajectory (Figure 6). As in the previous experiment, first the programmer drives the robot manually using a joystick to demonstrate the desired route to the robot and during this run, laser perception of the robot ($u_1 - u_{11}$) and the desired motor responses were logged every 250 ms.

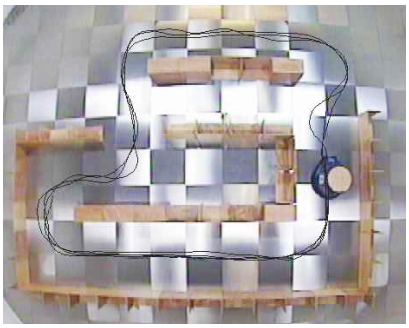

Fig. 6. Experiment 2. The desired route for the robot to learn. The programmer drives the robot manually, using a joystick to demonstrate the desired route to the robot

Having obtained the training data set, we used the K-means algorithm to divide the perception space of the robot into five clusters, A, B, C, D and E.

Figure 7 shows the graphical illustration of these five centroids.

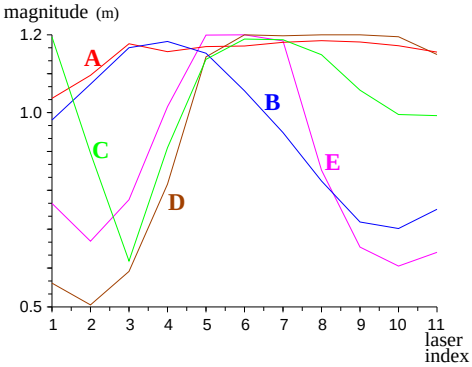

Fig. 7. Experiment 2. Graphical illustration of each centroid.

The internal map of the robot along the desired route which shows how the sensory data is clustered into 5 classes is illustrated in Figure 8.

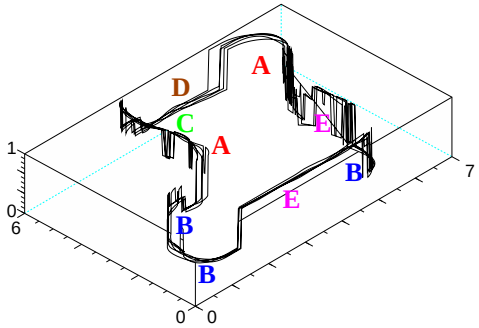

Fig. 8. Experiment 2. The internal map of the robot which clusters the environment into 5 different regions.

Once we had classified the sensory perception of the robot into distinctive classes, we then obtained one ARMAX model for each cluster, which links the laser readings ($u_1 - u_{11}$) of the robot to the desired angular velocity (ω) (to simplify the experiments, we clamped the linear velocity of the robot at 0.15 m/s). The models for each cluster A, B, C, D and E are given in Tables 2 and 3 respectively. These tables also present the error reduction ratio (ERR) value of each term presented in the polynomial, where the ERR values provide an indication of the contribution that each term in the model makes to the desired output variance.

Region A		**Region B**		**Region C**	
ERR	$\omega_A =$	ERR	$\omega_B =$	ERR	$\omega_C =$
0.00	-0.053	0.00	-0.477	0.00	$+1.208$
1.27	$-0.048 \cdot u_1(n)$	4.34	$-0.533 \cdot u_1(n)$	21.12	$-0.436 \cdot u_1(n)$
0.84	$-0.051 \cdot u_2(n)$	1.50	$+0.053 \cdot u_2(n)$	1.38	$-0.028 \cdot u_2(n)$
0.26	$+0.057 \cdot u_3(n)$	0.73	$+0.027 \cdot u_3(n)$	4.66	$+0.708 \cdot u_3(n)$
1.00	$-0.064 \cdot u_4(n)$	3.18	$-0.318 \cdot u_4(n)$	14.79	$-0.500 \cdot u_4(n)$
0.42	$-0.029 \cdot u_5(n)$	0.13	$+0.155 \cdot u_5(n)$	1.65	$-0.048 \cdot u_5(n)$
30.98	$-0.487 \cdot u_6(n)$	34.54	$+0.399 \cdot u_6(n)$	0.00	$+0.000 \cdot u_6(n)$
1.03	$+0.595 \cdot u_7(n)$	8.94	$+0.077 \cdot u_7(n)$	0.26	$+0.046 \cdot u_7(n)$
3.42	$+0.148 \cdot u_8(n)$	3.34	$+0.264 \cdot u_8(n)$	0.60	$-0.110 \cdot u_8(n)$
0.00	$+0.000 \cdot u_9(n)$	0.39	$+0.135 \cdot u_9(n)$	0.26	$+0.046 \cdot u_9(n)$
0.38	$+0.028 \cdot u_{10}(n)$	0.71	$-0.100 \cdot u_{10}(n)$	13.24	$-0.886 \cdot u_{10}(n)$
4.41	$-0.145 \cdot u_{11}(n)$	4.60	$+0.264 \cdot u_{11}(n)$	0.08	$-0.091 \cdot u_{11}(n)$

Table 2
Experiment 2. The polynomial ARMAX models which relate the laser readings of the robot (u_1 to u_{11}) to the angular velocity (ω) in regions A, B and C respectively.

Region D		**Region E**	
ERR	$\omega_D =$	ERR	$\omega_E =$
0.00	$+7.443$	0.00	-2.612
5.04	$-0.040 \cdot u_1(n)$	5.10	$+0.006 \cdot u_1(n)$
12.27	$+0.652 \cdot u_2(n)$	0.59	$+0.503 \cdot u_2(n)$
0.46	$-1.029 \cdot u_3(n)$	16.14	$+0.459 \cdot u_3(n)$
0.00	$+0.000 \cdot u_4(n)$	0.15	$-0.059 \cdot u_4(n)$
0.00	$+0.000 \cdot u_5(n)$	3.09	$+0.001 \cdot u_5(n)$
3.85	$-0.052 \cdot u_6(n)$	1.37	$+1.080 \cdot u_6(n)$
21.91	$-2.293 \cdot u_7(n)$	0.88	$+0.063 \cdot u_7(n)$
1.68	$-3.967 \cdot u_8(n)$	5.62	$+0.102 \cdot u_8(n)$
2.42	$+0.373 \cdot u_9(n)$	8.68	$+1.012 \cdot u_9(n)$
0.21	$+0.112 \cdot u_{10}(n)$	1.14	$+0.542 \cdot u_{10}(n)$
1.23	$-0.190 \cdot u_{11}(n)$	3.18	$-0.583 \cdot u_{11}(n)$

Table 3
Experiment 2. The polynomial ARMAX models which relate the laser readings of the robot (u_1 to u_{11}) to the angular velocity (ω) in regions D and E.

Model Validations Having obtained 5 polynomial ARMAX models, one for each cluster, we then tested them by letting them drive the robot in the training environment. Starting the robot anywhere along the desired trajectory, first the K-means algorithm classifies the environment according to the sensory perception of the robot. Once the robot recognizes the region it is in, it then selects the

correct polynomial obtained specifically for that region to drive the robot. Once the robot reaches the next region, the second polynomial is activated and the procedure goes on in this way.

The results show that the robot was successfull following the desired route without losing the track or crashing into obstacles. Note that when we tried to model the sensor-motor relationship with a *single* polynomial — rather than dividing the environment into subregions and obtaining one polynomial for each region — the resultant model failed to drive the robot successfully along the desired route.

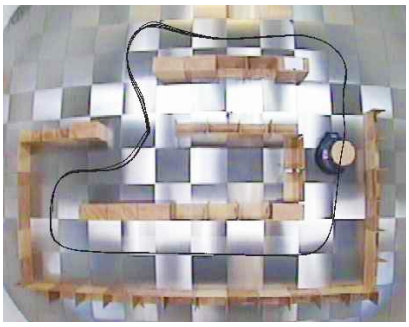

Fig. 9. Experiment 2. The trajectory of the robot under the control of the polynomial ARMAX models given in Tables 2 and 3.

3. Modelling Complex Robot Training Tasks through Bootstrapping System Identification

In the previous section we discussed that it is important to have information about the present state of the robot to determine the robot's next action. We therefore introduced a novel code generation method based on first recognizing distinctive landmarks in the environment, using unsupervised clustering algorithms, and then generating a different sensor-motor model for each landmark, using system identification.

However, it is possible that for some of these landmarks, the desired task is still too complex to be modelled with a direct link between raw sensory data and the motor response of the robot. In these cases it is common that the raw input readings are preprocessed with the aid of the programmer to extract higher level information from the sensory data in order to simplify the problem even further. However, preprocessing makes the code-generation process programmer-dependent, and as it is a manual, non-deterministic process, may result in suboptimal models.

We argue that it is important to have a formal, *algorithmic* method to extract high level input information, minimizing the use of human knowledge. We therefore propose a bootstrapping behaviour generation method which uses low level behaviours and the information about the current state of the robot to generate more complex ones. The method has three phases:

Phase 1 For obtaining simple sensor-motor controllers, we use the main modelling approach given in Section 1. Some examples of such low level reactive-controllers are obstacle-avoidance, door traversal, wall-following, etc.

Phase 2 The controllers obtained in phase 1 are loaded into the robot in order to form a behaviour repertoire in the robot's memory. We then obtain a NARMAX model, which models the new task as a function of these previously acquired behaviours. Here, the selection of behaviours is done using state variables which contain information about the state of the environment and the robot (see Figure 10).

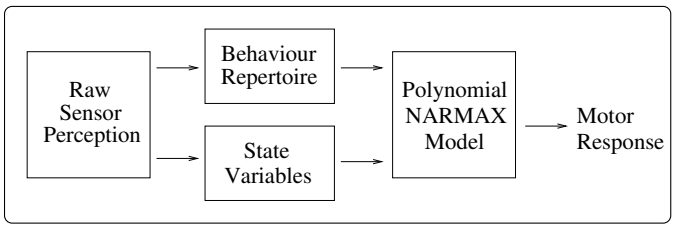

Fig. 10. The bootstrapping method of generating complex robot training tasks.

Phase 3 Once we have obtained the NARMAX model, we test it on the robot in order to validate its performance. If the new controller is successful it is added to the repertoire so that it can be used to generate even higher level controllers in the future.

The viability of the proposed method is demonstrated by a set of real robot experiments where a *Scitos G5* mobile robot was trained methodically to accomplish various sensor-motor tasks starting from simple obstacle avoidance to complex route learning.

3.1. *Experiment 3. Modelling Advanced Obstacle Avoidance Behaviour*

In the third experiment, we trained the robot to avoid obstacles towards the "obvious" side, as shown in Figure 11; if robot has more space on the right side, it turns to right, and if there is more space on the left, it turns to left.

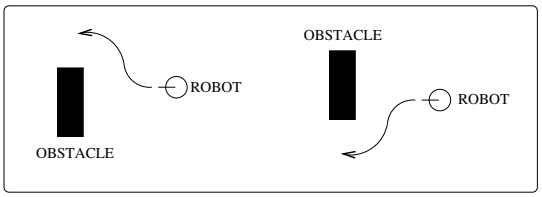

Fig. 11. Experiment 3. The desired obstacle avoidance behaviour.

To obtain the training data, the programmer drove the robot in the training environment (Figure 12) avoiding obstacles by turning the robot to the side having more space. During the experiments, the robot was started from the initial position S and stopped at the destination point F for

16 times. During each run, laser readings and the motor commands of the robot were logged in every 250 ms.

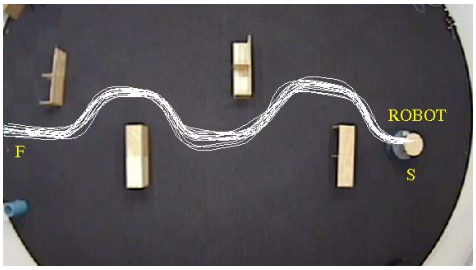

Fig. 12. Experiment 3. The trajectory of the robot, guided by the programmer. The robot was started from point S and avoided boxes along the route until it reached the destination point F.

Having obtained the training data, we coarse-coded laser readings into 11 sectors by averaging 62 readings for each 22° interval. Coarse-coded laser readings were clipped at 1.5 m to avoid models taking far-away obstacles into account, as these irrelevant to obstacle avoidance.

We then modelled the angular velocity ω_o of the robot as a function of coarse-coded laser readings $(u_1 - u_{11})$ using ARMAX system identification. The obtained model was a linear polynomial with 6 terms (Table 4).

$$\omega(n) = +0.183 - 0.187 \cdot u_4(n) - 0.137 \cdot u_5(n) \\ -0.021 \cdot u_6(n) - 0.045 \cdot u_7(n) + 0.265 \cdot u_8(n)$$

Table 4
Experiment 3. The ARMAX model which links the laser perception to the angular velocity of the robot to achieve advanced obstacle avoidance behaviour.

Model Validation We tested the steering speed model on the robot in three different test environments. During the experiments the linear speed of the robot was clamped to 0.1 m/s.

In the first test environment, the robot was started from 20 different initial positions in front of two boxes put next to each other and was expected to avoid them towards the "obvious" side. The results (Figure 13 show that the robot was able to avoid obstacles as desired [1] .

In the second (Figure 13b) and third (Figure 13c) test environments, we tested if the obtained angular speed model captured the real essence of obstacle avoidance behaviour. The robot was started in front of the boxes arranged to simulate a right and a left corner and in both cases the robot was successfull in avoiding the corners by turning the "obvious" side. Note that for both environment the robot was started from 16 different initial positions.

[1] In three runs out of 20 the robot was not able to choose a side and failed to escape from the boxes (visible in figure 13a). A possible solution to this problem would be to train a linear speed model as well.

(a) (b) (c)

Fig. 13. Experiment 3. The three environments where the obtained angular speed model ω_o given in table 4 was tested for obstacle avoidance behaviour.

3.2. *Experiment 4: Obstacle Avoidance based on Object Colour*

In a fourth experiment, we trained the robot in such a way that it determined the turning direction according to the colour of the obstacle, rather than choosing the "obvious" side: while the robot approaches an obstacle, it identifies the colour of the obstacle, and avoids red obstacles by a right turn, green obstacles by a left turn.

To obtain the training data set, we drove the robot in two environments. The first one contained boxes of red colour, resulting in right-turn obstacle avoidance (Figure 14a), the second environment contained green boxes, resulting in left-turn obstacle avoidance (Figure 14b). In each environment, we conducted the experiments 10 times starting the robot from initial point S, stopping at the final point F.

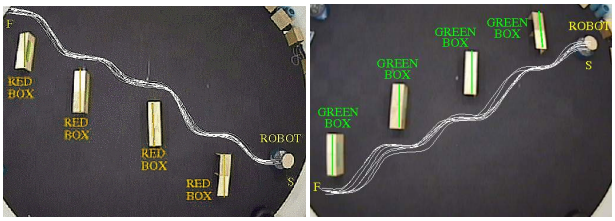

(a) (b)

Fig. 14. Experiment 4. The trajectories of the robot in two training environments. The first one, shown on the left, contained boxes of red colour, resulting in right-turn obstacle avoidance, the second environment, shown on the right, contained green boxes, resulting in left-turn obstacle avoidance.

During the experiments, we logged the coarse-coded laser readings and the motor responses of the robot as well as the colour index c_i ($c_i = 1$ for green, $c_i = 2$ for red boxes) of the closest obstacle to the robot every 250 ms.

After logging this perception-action data, we modelled the angular speed ω_t of the robot as a function of the coarse-coded laser readings $(u_1 - u_{11})$ and the colour index of the detected obstacle (c_i), using NARMAX system identification. The NARMAX model contained 21 terms (Table 5).

The resultant polynomial model ω_t is essentially the combination of two polynomials, where each polynomial turns the robot to a different direction, and the transition between the two is performed using the terms including state variable c_i (the last two rows in Table 5).

$$
\begin{aligned}
\omega_t(n) = &+3.839 - 0.661 \cdot u_4(n) - 0.212 \cdot u_5(n) \\
&+0.650 \cdot u_7(n) - 2.413 \cdot u_8(n) - 0.093 \cdot u_4(n)^2 \\
&+0.150 \cdot u_5(n)^2 - 0.002 \cdot u_7(n)^2 + 0.050 \cdot u_8(n)^2 \\
&-0.202 \cdot u_4(n) \cdot u_5(n) - 0.098 \cdot u_4(n) \cdot u_6(n) \\
&-0.546 \cdot u_4(n) \cdot u_7(n) + 1.121 \cdot u_4(n) \cdot u_8(n) \\
&-0.249 \cdot u_5(n) \cdot u_6(n) + 0.076 \cdot u_5(n) \cdot u_7(n) \\
&-0.129 \cdot u_6(n) \cdot u_7(n) + 0.130 \cdot u_6(n) \cdot u_8(n) \\
&-1.469 \cdot c_i(n) + 0.263 \cdot c_i(n) \cdot u_5(n) \\
&+0.369 \cdot c_i(n) \cdot u_6(n) + 0.280 \cdot c_i(n) * u_7(n)
\end{aligned}
$$

Table 5
Experiment 4. The NARMAX model for the angular speed of the robot for colour-encoded obstacle avoidance.

Model Validation As before we validated the performance of the obtained angular speed model by testing it on the robot. We put the robot in front of red and green boxes and let the model drive the robot. For each coloured box, the model was tested 16 times and the resultant trajectories of the robot are given in Figure 15. They confirm that the model given in Table 5 achieves the desired behaviour.

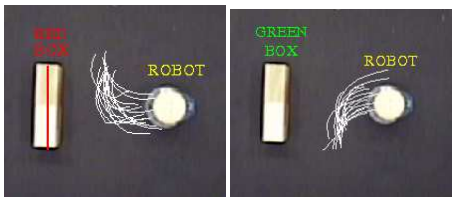

(a) (b)

Fig. 15. Experiment 4. The resultant trajectories of the robot guided by the angular speed model ω_t given in Table 4 when it is confronting the: (a) red coloured boxes and (b) green coloured boxes.

In order to quantify the performance of the angular speed model ω_t, we computed the strength of the association between the colour of the detected obstacle and the direction of the corresponding turning speed of the robot using *Cramer's V* test. To do so, we checked the sign of the resultant turning speed according to the colour of the detected obstacle during the test runs. When the robot detected a green obstacle, the resultant $\omega_t > 0$ (indicating to turn left) 97.651% of the time, and when the detected obstacle is red, $\omega_t < 0$ (indicating to turn right) 98.837% of the time. The results showed that there is a significant correlation ($V = 0.96$, note that V varies between 0 and 1, corresponding to "no association" and "perfect association" respectively).

3.3. *Experiment 5. Colour Encoded Route Learning Behaviour*

The previous experiment demonstrates how different behaviours can be embodied in a single polynomial where the transition between behaviours is done using state variables containing information about the current state of the environment. We will now show that this can be used to achieve more complex tasks.

Scaling up from the 3rd and 4th experiment, the fifth task was to generate a polynomial which can guide the robot to follow a particular route in order to reach a desired object. The experimental scenario is given in Figure 16, the environment is populated with red and green boxes in order to guide the robot to the destination point F, where the target object, a blue pillar, is present.

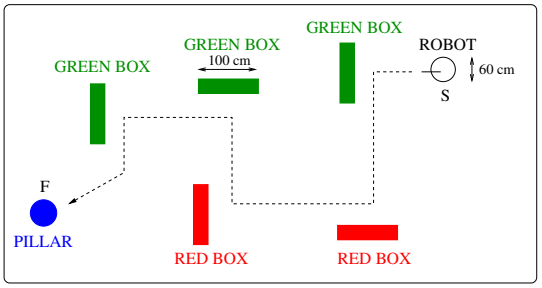

Fig. 16. Experiment 5. The experimental scenario where the desired task is to teach the robot to follow a particular route in order to reach the blue pillar at point F.

To collect the training data, the programmer drove the robot manually in the target environment (Figure 17) 10 times starting the robot from the initial position S and stopping the robot in front of the blue pillar (destination point F). During the training, laser readings, camera images and the motor commands of the robot were logged in every 250 ms.

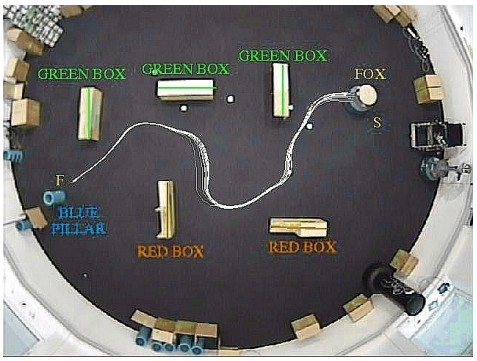

Fig. 17. Experiment 5. The trajectories of the robot guided manually by the human operator in order to obtain the training data.

Bootstrapping from Low-Level Controllers After logging the training data we processed the laser readings and the raw images to extract three low level controllers which were then be fed to the polynomial NARMAX models as inputs. These controllers are:

(i) **Obstacle avoidance controller** The first controller in the behaviour repertoire guides the robot to avoid obstacles. Here we used the polynomial model ω_o given in Table 4 obtained in experiment 3.

(ii) **Colour encoded turning controller** The second behaviour turns the robot to the right if the colour of the detected object is red, and to the left if the colour is green. Here we used the polynomial model ω_t given in table 5, obtained during experiment 4.

(iii) **Object seeking controller** We also implemented a simple object seeking controller which looks for the nearest object in front of the robot and guides the robot towards it.

Having identified the controllers, we also obtained three state variables which will help the system identification process to link the low level controllers to achieve the desired task:

(i) $\mathbf{d}_i$ defines if the target object is detected or not; $d = 0$ represents target object is not detected, and $d_i = 1$ represents target object is detected.

(ii) $\mathbf{o}_i$ defines if there is an obstacle close to the robot; $o_i = 0$ represents there is no obstacle detected, and $o_i = 1$ represents the presence of an obstacle.

(iii) $\mathbf{c}_i$ states the colour of the detected obstacle; $c_i = 1$ represents green, $c_i = 2$ represents red, and $c_i = 0$ represents all other colours.

We then obtained two polynomial models; one for the linear speed v_r and one for the angular speed ω_r of the robot — as a function of the predefined behaviours (ω_o, ω_t and ω_w) and the state variables (d_i, o_i and c_i) (Figure 18). The obtained models are given in Table 6.

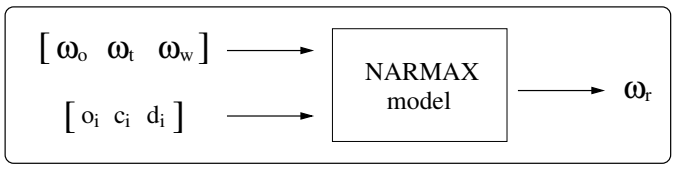

Fig. 18. Experiment 5. The bootstrapping method of generating complex route learning behaviour using predefined low level controllers; obstacle avoidance (ω_o), left/right turning (ω_t) and object seeking (ω_w). In order to link the behaviours we also present three state variables indicating the presence of the target object (d_i), presence of the obstacles (o_i) and the colour of the detected obstacles (c_i).

$$
\begin{aligned}
v_r(n) = {} & +0.100 - 0.100 \cdot d_i(n) \\
\omega_r(n) = {} & +0.100 \cdot d(n) + 1.000 \cdot \omega_w(n) \\
& -1.000 \cdot o_i(n) \cdot \omega_w(n) + 1.000 \cdot o_i(n) \cdot \omega_o(n) \\
& -1.000 \cdot o_i(n) \cdot c_i(n) \cdot \omega_o(n) + 1.000 \cdot o_i(n) \cdot c_i(n) \cdot \omega_t(n) \\
& +1.000 \cdot d_i(n) \cdot o_i(n) \cdot \omega_w(n) - 1.000 \cdot d_i(n) \cdot o_i(n) \cdot \omega_o(n) \\
& +1.000 \cdot d_i(n) \cdot o_i(n) \cdot c_i(n) \cdot \omega_o(n) \\
& -1.000 \cdot d_i(n) \cdot o_i(n) \cdot c_i(n) \cdot \omega_t(n)
\end{aligned}
$$

Table 6
Experiment 5. The polynomial models for the linear v_r and angular speed ω_r of the robot.

3.3.0.1. *Model Validation* Having obtained the perception models v_r and ω_r, we tested them on the robot. We let the models drive the robot in the target environment 10 times. Figure 19 shows the resultant trajectories, where in each run the robot was successful to reach the target object.

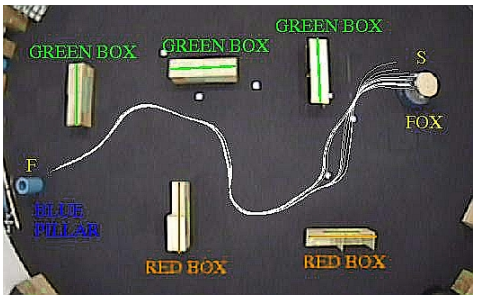

Fig. 19. Experiment 5. The trajectories of the robot under the control of the perception models given in Table 6.

3.4. *Extended Bootsrapping Method*

In experiment 3 we demonstrated how simple NARMAX models can be used to achieve more complex tasks. One interesting question here is "what happens if the low level controllers found in the behaviour repertoire are not adequate to generate the desired task?"

To address this question, we extended the proposed method by adding raw sensory perception to the modelling process. In this way, we let the polynomial model combine raw sensory data with the low-level controllers automatically. Again, the transition between the controllers and the raw sensory data is controlled according to the state of the environment and the robot (Figure 20).

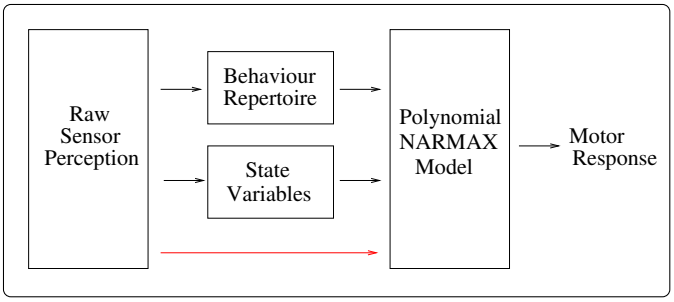

Fig. 20. The extended bootstrapping method of generating complex robot training tasks. In the extended version we also give raw sensory data as inputs to the system.

3.5. *Experiment 6. Complex Route Following combined with Door Traversal Behaviour*

To demonstrate the extended method, we taught the robot to follow a complex route of different stages (Figure 21). First, the robot has to reach a blue pillar by correctly following the coloured objects. Once it reaches the

pillar, it has to wait with zero linear and angular speeds until the pillar is removed from the environment (stage 2). Once the pillar is removed, the robot must complete the route by traversing the two consecutive door-like openings to reach the destination point F.

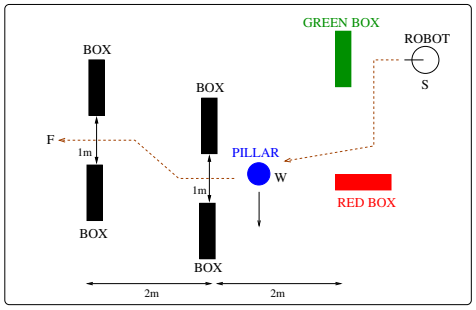

Fig. 21. Experiment 6. The experimental scenario for the desired complex route learning task.

As before we obtained the training data by driving the robot manually in the target environment shown in Figure 22. Starting the robot at initial position S, first we drove the robot to point W. Then the robot was stopped in front of the pillar until the pillar was removed by the human operator. We then continued driving the robot to pass through two consecutive door-like openings. The experiments were repeated 10 times and for each run we logged the laser perception, camera images and the motor commands of the robot in every 250 ms.

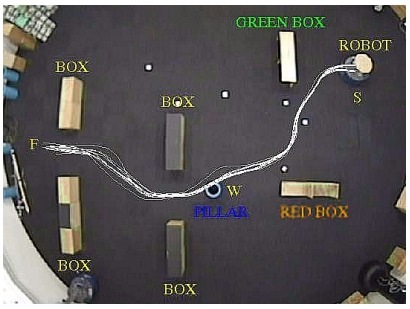

Fig. 22. Experiment 6. The trajectories of the robot under the manual control of the human operator for training data collection.

Obtaining Sensor Based Models After logging the training data, we fed the raw perception data to low-level controllers present in the behaviour repertoire of the robot to generate higher level inputs for the desired task. But this time we also coarse-coded the laser readings into 11 sectors ($u_1 - u_{11}$) by averaging 62 readings for each 22° in order to enrich the system inputs, since there is no dedicated door traversing controller in the behaviour repertoire of the robot. Also for the transition between the behaviours, we computed a state flag s_i which indicates if the blue pillar is removed from the front of the robot ($s_i = 1$) or not ($s_i = 0$).

We then obtained two NARMAX models, expressing v_c and ω_c as a function of coarse-coded laser readings ($u_1 \dots u_{11}$), route following controllers v_r and ω_r obtained in Section 3.3, and state variable s_i. The obtained models are given in Table 7.

$$
\begin{aligned}
v_c(n) = {} & +v_r + 0.1 \cdot s_i(n) \\
\omega_c(n) = {} & -0.033 + 1.016 \cdot \omega_r(n) + 0.144 \cdot u_4(n) \\
& -0.088 \cdot u_5(n) + 0.004 \cdot u_6(n) - 0.131 \cdot u_7(n) \\
& +0.014 \cdot u_8(n) + 0.208 \cdot \omega_r^2(n) - 0.026 \cdot u_4^2(n) \\
& +0.029 \cdot u_5^2(n) + 0.062 \cdot u_7^2(n)^2 - 0.025 \cdot u_4(n) \cdot u_8(n) \\
& +0.394 \cdot s_i(n) - 1.051 \cdot s_i(n) \cdot \omega_r(n) \\
& -0.145 \cdot s_i(n) \cdot u_4(n) - 0.060 \cdot s_i(n) \cdot u_5(n) \\
& -0.040 \cdot s_i(n) \cdot u_6(n) + 0.026 \cdot s_i(n) \cdot u_7(n)
\end{aligned}
$$

Table 7
Experiment 6. The polynomial models for the linear and angular speed of the robot for complex route learning and door traversal behaviour. The last three rows show the terms including state variable s_i.

Model Analysis and Validation Once we obtained the sensor based models, we used them drive the robot in the target environment in order to validate the performance. Figure 23 shows the trajectories of the robot for 10 runs, where the robot completed the track successfully in each attempt.

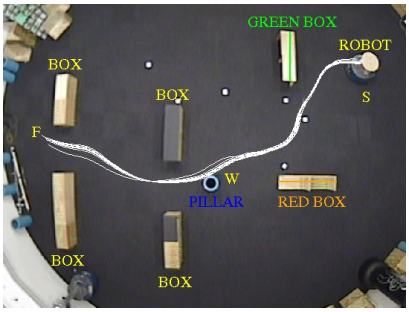

Fig. 23. Experiment 6. The trajectory of the robot under the control of the perception models given in Table 7.

Transparent Models Having transparent models like the ones given in Table 7 has a number of advantages, for example the possibility to analyse the robot behaviour formally. Here, for instance, one can see that the model of Table 7 ω_c has two components. The first one is the colour-based route following behaviour which was previously obtained in section 3.3, taking the control of the robot when state flag s_i equals 0. The second behaviour is a door traversal controller activated when $s_i = 1$.

The separability of the behaviours enabled us to add door traversal controller to the behaviour repertoire of the robot. In this way we do not only obtain models to achieve the desired task, but we also extract new low level controllers from the polynomial model in order to enrich the behaviour repertoire of the robot.

4. Conclusion

This paper demonstrates, in theory and practical robotics experiments, how system identification can be used to generate *complex* robot training tasks, i.e. tasks that are context-dependent, and require memory for successful completion. Those tasks cannot normally represented by a *single* model, and we show how several models can be combined into one by a simple bootstrapping method.

In Section 2, we emphasize the importance of detecting these transitions and propose a novel method to estimate them. The method relates distinctive locations in the environment to the state of the robot, using an unsupervised clustering algorithm.

Once we estimate the current state of the robot accurately, the next step is to combine this state information with the perception of the robot to generate the essential motor commands, to accomplish the desired complex robot training tasks. One way of addressing this issue is to generate a separate sensor-motor couplings for each state of the robot. The viability of this method has been demonstrated by modelling right wall following and complex route learning behaviours.

However there are cases where for some of these landmarks, the desired task is still too complex to be modelled with a direct link between raw sensory data and the motor response of the robot. Therefore, in Section 3, we introduce a bootstrapping method of generating complex robot training tasks using polynomial NARMAX structures. The method is based on obtaining hierarchical polynomial models which model the desired task by combining predefined low level sensor motor controllers and raw sensory data.

This allows us to combine different low level controllers in a single polynomial to achieve more complex tasks. The transition between these controllers is done using state variables which contain information about the state of the environment. To demonstrate the viability of the proposed method, we generated a complex route following polynomial which computes the desired motor responses of the robot based on the inputs from low level controllers (such as obstacle avoidance and colour encoded turning controllers).

The method also allows as to combine the raw sensory data of the robot with the previously defined low level controllers. This does not only produce robust high level controllers to achieve the desired task, but also enables us to extract new low-level controllers from the generated controller. The obtained polynomial model for the complex route learning behaviour includes a door traversal controller generated automatically using raw sensory data for the second part of the desired route.

Future Work In Section 2, we estimate the the state of the robot based on its current sensory perception assuming that state information is observable through robot sensors.

However there are cases where multiple states are indistinguishable to the robot because of the perceptual similarities (perceptual aliasing [26]).

In these kind of situations, state estimation can not be based on only the current sensory perception of the robot, but some extra information is needed. One way of dealing with the perceptual aliasing problem is to incorporate an expectation model — a model which estimates the next state of the robot based on the previous states and the actions of the robot — into the recognition of locations (Figure 24). With the incorporation of the expectation model, the robot would have a rough idea about which state it is going to and would be able to combine this information with its current sensory readings to estimate the next state accurately. Therefore we are currently investigating ways of developing a formal method to obtain expectation models automatically and incorporating them into the state estimation process.

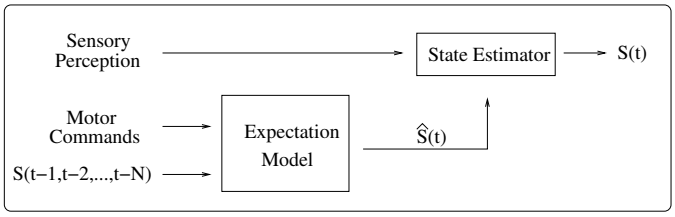

Fig. 24. The incorporation of the expectation model to the process of estimating the current state of the robot. The expectation model predicts the next state $\hat{S}(t)$ of the robot, based on the previous states and the actions of the robot. The state estimation model then combines the current sensory readings of the robot with the expected state information to predict the next state $S(t)$ of the robot.

Furthermore we are working on the integration of the state estimation process with robot training and the NARMAX system identification methods in a single framework in order to develop a formal method of generating complex robot training tasks automatically and algorithmically without needing explicit knowledge of robot programming. The work already carried out and that proposed forms part of our ongoing research in universities of Ulster, Essex and Sheffield.

Acknowledgments

We express our thanks to Emre Özbilge for his contribution to the experimental work presented in this paper.

References

[1] U. Nehmzow, *Mobile Robotics: A practical introduction*, 2nd ed. Springer Verlag, 2003.

[2] ——, "Quantitative analysis of robot-environment interaction – towards "scientific mobile robotics"," *International Journal of Robotics and Autonomous Systems*, vol. 44, pp. 55–68, 2003.

[3] U. Nehmzow and K. Walker, "The behaviour of mobile robot is chaotic," *AISB Journal*, vol. 1(4), pp. 373–388, 2003.

[4] T. Kyriacou, U. Nehmzow, R. Iglesias, and S. A. Billings, "Task characterization and cross-platform programming through system identification." *International Journal of Advanced Robotic Systems*, vol. 2, pp. 317–324, 2005.

[5] R. Iglesias, T. Kyriacou, U. Nehmzow, and S. Billings, "Robot programming through a combination of manual training and system identification," in *Proc. of ECMR 05 - European Conference on Mobile Robots 2005*. Springer Verlag, 2005.

[6] U. Nehmzow, O. Akanyeti, C. Weinrich, T. Kyriacou, and S. Billings, "Robot programming by demonstration through system identification," in *IROS*, San Diego, USA, 2007.

[7] O. Akanyeti, U. Nehmzow, C. Weinrich, T. Kyriacou, and S. Billings, "Programming mobile robots by demonstration through system identification," in *ECMR*, Freiburg, Germany, 2007.

[8] S. Lauria, G. Bugmann, T. Kyriacou, J. Bos, and E. Klein, "Training personal robots using natural language instruction," *IEEE Intelligent System*, vol. 16, pp. 38–45, 2001.

[9] A. Dearden and Y. Demiris, "Learning forward models for robots," in *Proceedings of the International Joint Conference on Artificial Intelligence*, Edinburgh, UK, 2005, pp. 1440–1445.

[10] A. Billard and G. Hayes, "Learning to communicate through imitation in autonomous robots," in *In 7th International Conference on Artificial Neural Networks*. Springer-Verlag, 1997, pp. 763–768.

[11] O. Akanyeti, U. Nehmzow, and S. Billings, "Robot training using system identification," *Int. J. Robotics and Autonomous Systems*, 2008, (in press).

[12] R. Iglesias, U. Nehmzow, and S. Billings, "Model identification and analysis in robot training," in *Proc. of TAROS 2007, (Towards Autonomous Robotic Systems)*. Springer Verlag, 2007, pp. 40–47.

[13] P. Eykhoff, *System Identification: parameter and state estimation*. London: Wiley-Interscience, 1974.

[14] ——, *Trends and Progress in System Identification*. Pergamon Press, 1981.

[15] S. Chen and S. Billings, "Representations of non-linear systems: The narmax model," *International Journal of Control*, vol. 49, pp. 1013–1032, 1989.

[16] S. Billings and S. Chen, "The determination of multivariable nonlinear models for dynamical systems," in *Neural Network Systems, Techniques and Applications*, C. Leonides, Ed. Academic press, 1998, pp. 231–278.

[17] I. Sobol, "Sensitivity estimates for nonlinear mathematical models," *Mathematical Modelling and Computational Experiments (MMCE)*, vol. 1, pp. 407–414, 1993.

[18] K. Chan, A. Saltelli, and S. Tarantola, "Sensitivity analysis of model output: Variance-based methods make the difference," in *Proc. of 1997 Winter Simulation Conference, (Towards Autonomous Robotic Systems)*, 1997, pp. 261–268.

[19] R. Iglesias, U. Nehmzow, T. Kyriacou, and S. Billings, "Modelling and characterization of a mobile robot's operation," in *CAEPIA 2005, 11th conference of the Spanish association for Artificial Intelligence*, Santiago de Compostela, Spain, 2005.

[20] A. Saltelli, K. Chan, and E. M. Scott, *Sensitivity analysis.* Wiley, 2000.

[21] U. Nehmzow, O. Akanyeti, and S. Billings, "A proposal of a methodology for the analysis of robot-environment interaction through system identification," in *TAROS*, Edinburgh, Scotland, 2008.

[22] U. Nehmzow, *Robot Behaviour — Design, Description, Analysis and Modelling*. Heidelberg, New York, London: Springer, 2009.

[23] O. Akanyeti, T. Kyriacou, U. Nehmzow, R. Iglesias, and S. Billings, "Visual task identification and characterization using polynomial models," *Int. J. Robotics and Autonomous Systems*, vol. 55, pp. 711–719, 2007.

[24] H. I. Christensen, "Slam paper repository," 2005. [Online]. Available: http://www.cas.kth.se/SLAM/slam-papers.html

[25] J. B. MacQueen, "Some methods for classification and analysis of multivariate observations," in *Proc. of 5-th Berkeley Symposium on Mathematical Statistics and Probability*, Berkeley, USA, 1967, pp. 281–297.

[26] S. D. Whitehead and D. H. Ballard, "Learning to perceive and act by trial and error," *Machine Learning*, vol. 7(1), pp. 45–83, 1991.